

2

DTIC FILE COPY

AD-A181 095

2006 0524 000

DEVELOPMENT OF AN OPTICAL
 SURVIVABILITY COATING

Final Technical Report: Phase I

DTIC
 ELECTE
 JUN 04 1987
 S D

DISTRIBUTION STATEMENT A
 Approved for public release
 Distribution Unlimited



CVD Incorporated

185 NEW BOSTON STREET, WOBURN, MA 01801

87 5 5 002

2

CVD TR-9076

DEVELOPMENT OF AN OPTICAL
SURVIVABILITY COATING

Final Technical Report: Phase I

April 29, 1987

Contract No. DASG60-86-^c0072

DTIC
ELECTE
JUN 04 1987
S D
D

Prepared for

U.S. ARMY STRATEGIC DEFENSE COMMAND
P.O. Box 1500
Huntsville, AL 35807-3801

Prepared by

CVD INCORPORATED
185 New Boston Street
Woburn, MA 01801

DISTRIBUTION STATEMENT A
Approved for public release;
Distribution Unlimited

TABLE OF CONTENTS

<u>Section</u>		<u>Page</u>
1.0	INTRODUCTION	1
2.0	PHASE I RESULTS	4
	2.1 CVD ZnS _x Se _{1-x} Rugate Process	4
	2.2 Experimental Results	10
3.0	DISCUSSION OF RESULTS	30
4.0	CONCLUSIONS AND RECOMMENDATIONS	32
	REFERENCES	33



Accession For	
NTIS CRA&I	<input checked="" type="checkbox"/>
DTIC TAB	<input type="checkbox"/>
Unannounced	<input type="checkbox"/>
Justification	
By <i>ltr. on file</i>	
Distribution /	
Availability Codes	
Dist	Availability and/or Special
<i>A-1</i>	

LIST OF FIGURES

<u>Figure</u>		<u>Page</u>
1	Comparison of indices of refraction of CVD ZnS and ZnSe	5
2	Mole fraction of ZnS in alloy ZnS_xSe_{1-x} plotted vs. gas phase composition expressed as the ratio of the flow rate of H_2S gas (Q_{H_2S}) over the total flow rate of $H_2S + H_2Se$ gas ($Q_{H_2S} + Q_{H_2Se}$).	8
3	Schematic of research CVD apparatus used to deposit ZnS_xSe_{1-x} rugates.	11
4	Location of ZnSe and ZnS substrates in Run #1.	15
5	Transmission of ZnS_xSe_{1-x} rugate film material from Run #1 taken from exhaust end of mandrel plate (see Fig. 3).	16
6	Transmission of ZnS_xSe_{1-x} rugate filter deposited on ZnSe sample 1-1A (see Fig. 4) during Run #1.	17
7	Location of ZnSe and ZnS substrates in Run #3.	20
8	Infrared transmission of rugate filter grown on sample #3-2A during Run #3. See Fig. 7 for location of sample in deposition zone. Curve (1) is for gain of unity; Curve (2) gain of 2x; Curve (3) gain of 3x.	21
9	Infrared transmission of rugate filter grown on sample #3-9A during Run #3. See Fig. 7 for location of sample in deposition zone.	22
10	Photograph of an etched surface of rugate filter parallel to deposition axis on sample #3-1A in Run #3. Note the periodic line pattern showing that the concentration of ZnSe and ZnS is changing periodically along the deposition axis.	23

LIST OF FIGURES (Cont'd)

<u>Figure</u>		<u>Page</u>
11	Location of ZnSe substrates in Run #4.	25
12	Infrared transmission of ZnS_xSe_{1-x} rugate filter on ZnSe substrate sample #4-3A in Run #4. See Fig. 9 for location of sample in deposition zone. Curve (1) is for gain of unity; Curve (2) gain is 2x; Curve (3) gain is 3x.	26
13	Infrared transmission of ZnS_xSe_{1-x} rugate filter on ZnSe substrate samples #4-1A in Run #4. Curve (1) is for a film thickness of 250 μm and Curve (2) is for a thickness of 900 μm .	27
14	Photograph of etched surface, parallel to deposition axis, for sample #4-3A. Note the dark-light lines showing the periodic structure of the film and sudden change in growth morphology (cone structure). We believe this phenomena is due to the impurities being swept onto the surface of the film during growth.	29

LIST OF TABLES

<u>Table</u>		<u>Page</u>
1	Deposition of Filter Parameters of ZnS_xSe_{1-x} Rugate Filter Runs	14

1.0 INTRODUCTION

A critical objective of the Strategic Defense Initiative (SDI) is the development of optical, particularly infrared, techniques to detect, acquire and track space objects and ballistic missiles. In order for the infrared (IR) systems to detect these relatively cool objectives at suitable ranges (1000 km or more), it is necessary that they operate at the limit of detectivity. Such high sensitivity makes these systems very vulnerable to laser counter measures. Particularly sensitive are the focal plane detectors, focusing optics and optical coatings, all of which have relatively low, optical damage thresholds.

In addition to these SDI requirements, many current tactical IR systems employed on high performance aircraft and various missiles are also vulnerable to directed energy weapons. One hardening technique that can be used to protect these optical systems is to place a filter at an appropriate position in the optical train which will absorb the narrow band laser energy but otherwise transmit the wide band infrared signals. These notch, blocking filters must clearly possess a higher laser damage threshold than the components they are to protect. This requirement can sometimes be achieved by positioning the filter near the aperture of the collecting optics before the laser energy has been appreciably focused and its intensity or fluence increased. However, this necessitates that the filter be of large area, i.e., of the diameter of the telescope.

The conventional approach to produce such filters has been to use the multilayer dielectric stack. However, such filters, composed of many discrete layers of dissimilar materials, are vulnerable to mechanical and thermal stress resulting from the differences in thermal expansion coefficients, residual stress and adherence of the individual layers. Interfaces between the layers can trap impurities which result in the absorption of radiation and, thereby, reduce the tolerance of the filters to high radiation fluxes. Furthermore, the abrupt interfaces become sites of high dislocation densities which degrade laser hardening performance by scattering radiation into the sensor.

Besides the above mechanical and thermal problems, the discrete layer approach also has some optical disadvantages. The step-function nature of the index profile inevitable results in reflectance peaks at undesired wavelengths and subsequently reduces the amount of signal available to the detector. This problem is compounded in a multinotch filter, where several wavelengths must be rejected. Multilayer technology requires the stacking of filters, which results in a separate and additive see-through penalty from the sidebands of each filter element.

A solution of these problems is offered by the rugate filter, whose material composition (and therefore its refractive index) varies continuously within the filter structure. In particular, the rugate filter can be designed to provide a high protection level for sensitive detector systems. Continuous variation of material composition reduces stresses arising from mismatch of thermal expansion coefficients and lattice constants at the abrupt interfaces. In the extreme case of very small compositional variations, the filter properties approach those of a homogeneous medium. Compositional grading also makes possible sinusoidal refractive index profiles that result in sideband-free reflectance spectra and, hence, improve signal transmission. The rugate approach is appropriate for single-step fabrication of multi-line filters. By fabricating a refractive index profile which is the linear superposition of a number of sine functions of different periods, a high see-through filter with multiline protection is produced. Compositional grading is also expected to improve the optical properties of filters by eliminating the deleterious effects of discrete interfaces discussed above.

Implementation of rugate technology requires techniques for precise compositional control of the filter material. Real-time, in-situ monitoring and feedback control systems capable of dealing with films having continuously varying refractive indices are a critical requirement to assure precise control of film growth and to achieve theoretical optical performance limits.

Several novel approaches to the design and fabrication of rugate (graded refractive index) filters were proposed at the 1982 Monterey Conference

on Laser VEH.¹⁻³ These filters offer significant advantages over the conventional quarter wavelength dielectric stack filters in that multiple (laser) lines can be rejected with a single layer rugate with very narrow rejection bandwidths and high-out-of-band pass-through. Rugates also offer the potential for wide angle rejection and the possibility of increased laser damage thresholds due to the elimination of discontinuous material interfaces. Rugates thus show the promise of being used extensively in future optical systems.

2.0 PHASE I RESULTS

As stated in our Phase I proposal, the primary technical objective of this Phase I effort was to establish the CVD conditions necessary to produce the required index profile that yield narrow-band, high-optical density, rugate filters by the codeposition of ZnS and ZnSe. We did not plan to produce any rugate filters during this Phase I program, however, in the time between writing our Phase I proposal and the award of our Phase I contract, we acquired additional analytical and experimental evidence through both in-house and government sponsored research which we felt was sufficient to attempt producing high optical density (O.D.) rugate filters. These results are discussed below.

2.1 CVD ZnS_xSe_{1-x} Rugate Process

A rugate filter refers to a thin film filter with a continuously varying refractive index designed to be highly reflective at one or more wavelengths while transmitting the others in a given spectral region, e.g. visible and/or IR. The material interface of conventional multilayer stacks are effectively eliminated.

Our technical approach to produce high optical density (OD) rugate filters is as follows: zinc sulfide (ZnS) and zinc selenide (ZnSe) are widely employed infrared transmissive materials. ZnS and ZnSe also possess different indices of refraction throughout their useful spectral region, as is shown in Fig. 1. These two substances are also completely miscible in the crystalline form, i.e., the alloy, ZnS_xSe_{1-x}, exists for 0 ≤ x ≤ 1. Therefore, a mixture of ZnS and ZnSe will have an index which closely corresponds to the sum of the pure indices weighed by their molar composition. This relationship between chemical composition and refractive index is theoretically expected to hold in spectral regions removed from anomalous dispersion and has been verified experimentally by CVD Inc.

In a previous program, supported by the U.S. Army Missile and Guidance Directorate, Redstone Arsenal, Huntsville, AL under Contract No.

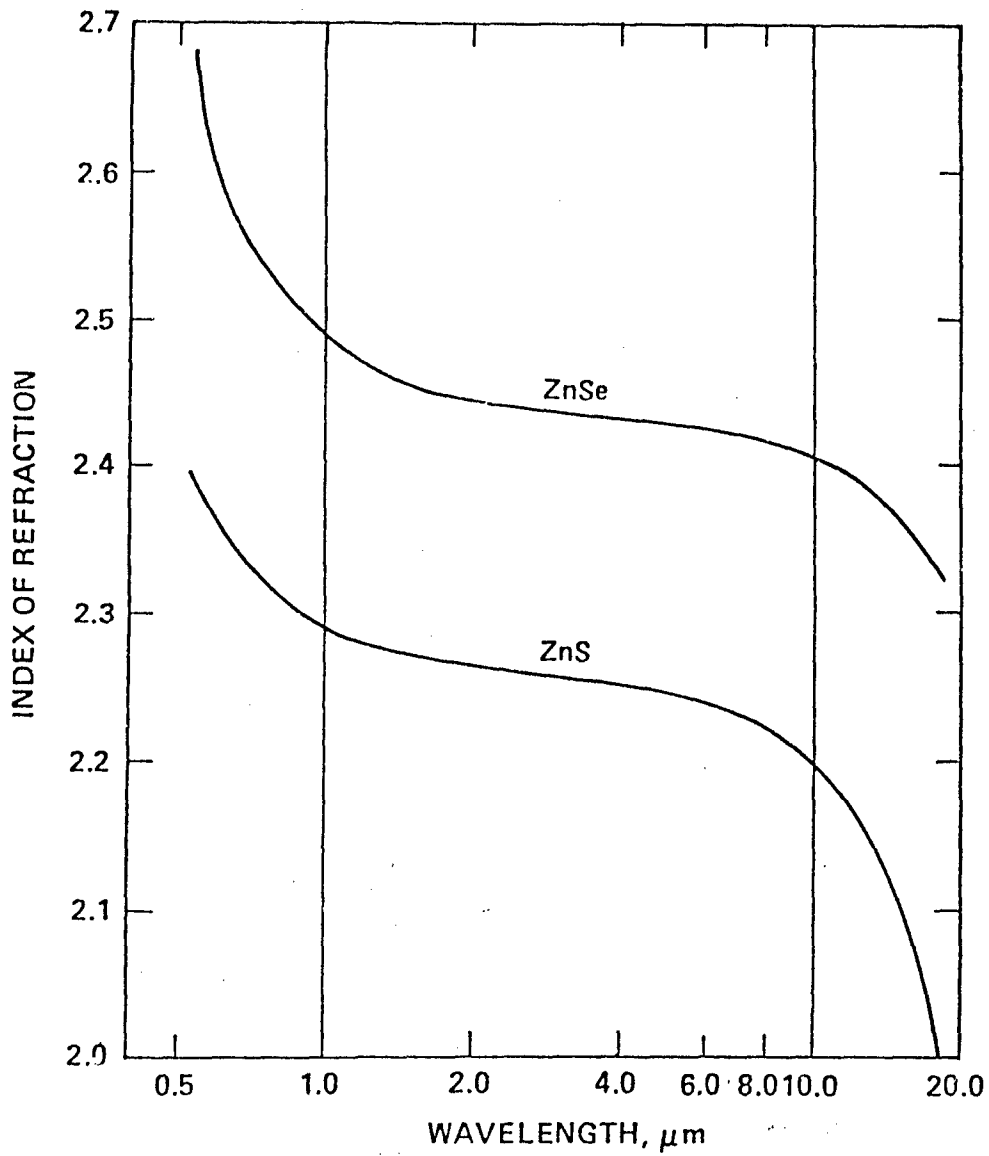


Figure 1. Comparison of indices of refraction of CVD ZnS and ZnSe.

DAAH01-84-C-0084, CVD Inc. demonstrated the feasibility of producing an infrared (IR) gradient index (GRIN) material from the alloy ZnS_xSe_{1-x} by co depositing ZnSe and ZnS in a controlled CVD process.⁴ To produce material with a known and predictable refractive-index profile, it is necessary to control the solid composition of the alloy, its refractive index and the deposition rate as a function of time during the CVD process. In order to define the function relationships between the various parameters, an analytical model of the CVD process was developed, and experiments were performed to verify the model.

From this work we were able to establish that the refractive index, n , of the alloy, ZnS_xSe_{1-x} , was given by,

$$n = n_{ZnSe} (1-x) + n_{ZnS} (x) \quad (1)$$

where n_{ZnSe} and n_{ZnS} are the refractive indices of ZnSe and ZnS respectively, and x is the mole fraction of ZnS in the solid alloy, ZnS_xSe_{1-x} . Next, using a simple kinetic model of the deposition process, the rates of formation, R , of ZnSe and ZnS on the substrate surface were assumed to be independent of each other and given by the Arrhenius expressions of the type,

$$R_{ZnSe} = P_{H_2Se} A_1 \exp(-E_{a1}/k_B T) = k_1 \cdot P_{H_2Se} \quad (2)$$

$$R_{ZnS} = P_{H_2S} A_2 \exp(-E_{a2}/k_B T) = k_2 \cdot P_{H_2S} \quad (3)$$

where P_{H_2Se} and P_{H_2S} are the partial pressures of H_2Se and H_2S , respectively, above the substrate surface, A_1 and A_2 are constants, E_{a1} and E_{a2} are the activation energies of formation of ZnSe and ZnS, k_1 and k_2 are the corresponding rate constants, k_B is Boltzmann's constant and T is the temperature. Dividing Eq. (2) by Eq. (3) and assuming the partial pressures of H_2Se and H_2S are proportional to their flow rates, Q_{H_2Se} and Q_{H_2S} , we can derive an expression for x , the mole fraction of ZnS in the solid alloy as a function of the gas phase composition,

$$x = \left[\left(\frac{Q_{H_2Se}}{Q_{H_2S}} - 1 \right) \frac{k_1}{k_2} + 1 \right]^{-1}, \quad (4)$$

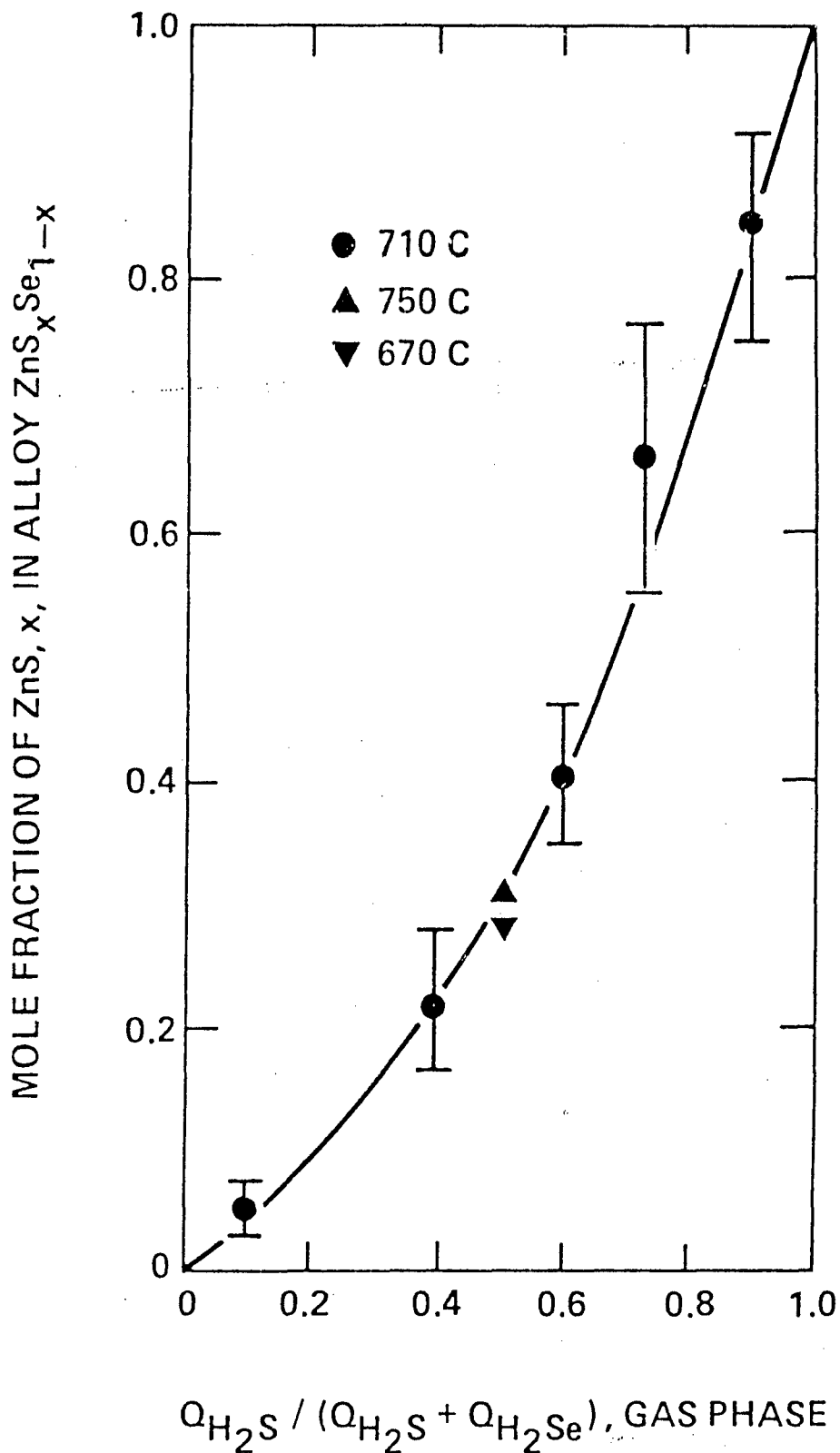


Figure 2. Mole fraction of ZnS in alloy ZnS_xSe_{1-x} plotted vs. gas phase composition expressed as the ratio of the flow rate of H_2S gas (Q_{H_2S}) over the total flow rate of $H_2S + H_2Se$ gas ($Q_{H_2S} + Q_{H_2Se}$).

$$BW \cong \frac{2\Delta n}{\pi n_a} \quad (6)$$

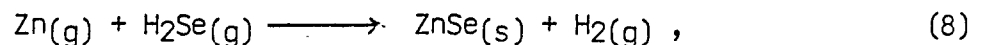
$$OD \cong 0.43 \frac{\pi}{2} (BW) \ell - 0.6 \quad (7)$$

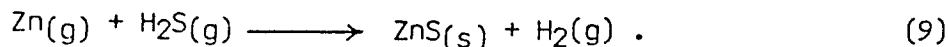
where BW is the bandwidth, Δn is the amplitude of the index variation, n_a is the average (mean) refractive index, OD is the optical density of the filter defined as $\log_{10}(I^{-1})$, where I is the transmission at the rejection wavelength, and ℓ is the number of cycles.

Equations (6) and (7) can be used to determine the index variation and number of cycles required to produce a rugate filter of specific bandwidth and optical density. For example, consider a ZnS_xSe_{1-x} rugate filter with a rejection wavelength of $\lambda = 10 \mu m$, a bandwidth of 5% and an optical density of 5. The refractive index of pure ZnSe at $10 \mu m$ is 2.407 and for ZnS it is 2.201, therefore, if we let $n_a = 2.303$, the required Δn would be 0.181 units and the number of cycles required would be 166. Since the optical period is $5 \mu m$, the thickness of each cycle would be $5/n_a = 2.17 \mu m$, and the total thickness of the film would be $360 \mu m$.

This example illustrates the importance of being able to grow very thick films to achieve high optical density filters. This is especially true at larger wavelengths, i.e., in the IR, due to the large period ($\lambda/2$). Notice in Eq. (6) and (7) that as the bandwidth decreases, the number of cycles needed to achieve a specific OD will increase. Therefore, for narrow stopband filters of high OD, very thick films will be required, i.e., up to $1000 \mu m$. In this Phase I effort we concentrated on producing rugate filters in the wavelength region from 7-11 μm .

The CVD process we used to deposit ZnS_xSe_{1-x} rugate filters involved the following chemical reactions,





Here the subscripts g and s refer to the gaseous and solid species. In our process we keep the flow rate of Zn vapor constant during the entire film growth deposition. The flow rates of H₂S and H₂Se gases are varied during the process to achieve a sinusoidal index variation in the solid alloy, ZnS_xSe_{1-x}.

2.2 Experimental Results

A CVD research furnace was modified to perform depositions of various rugate filters. A schematic of this apparatus is shown in Fig. 3. It consists of a Model 5400 Lindberg three-zone, horizontal, resistively heated, tube furnace modified with a chamber to perform CVD reactions. The temperature of the central zone is 200-1200 ± 0.5 C over an 0.45 cm length. The inside working diameter of the furnace is 18 cm. The retort (right hand) zone is used to heat a graphite crucible containing Zn metal to be volatilized as a source of gaseous Zn. The metal vapors are carried into the reaction (middle) zone by argon carrier gas and enter the reaction zone at low velocity through four holes located symmetrically around the H₂S/H₂Se injector. The H₂S and H₂Se gases (also used with argon) are introduced as a high velocity jet producing a recirculation zone along the substrate surface. Mixing of the Zn, H₂S and H₂Se gases occurs in the recirculation zone. To prevent premature decomposition, the H₂S/H₂Se injector is water-cooled. The deposition zone is maintained at a higher temperature (~ 700 C) than the Zn retort (~ 600 C) to prevent condensation of the Zn in the deposition zone. The exhaust (left-hand) zone is maintained at a low temperature to assure condensation of most of the unreacted Zn. The remaining unreacted gases pass through filters, the vacuum pump and KOH scrubbers before exhausting to the atmosphere. Since H₂Se and H₂S are highly toxic, care must be exercised in their use. The exhaust scrubber system is designed for efficient removal of these gases.

The H₂S and H₂Se gas flow rates are controlled by mass flow meters to assure constant and reproducible flow rates. The Zn flow rate is maintained by

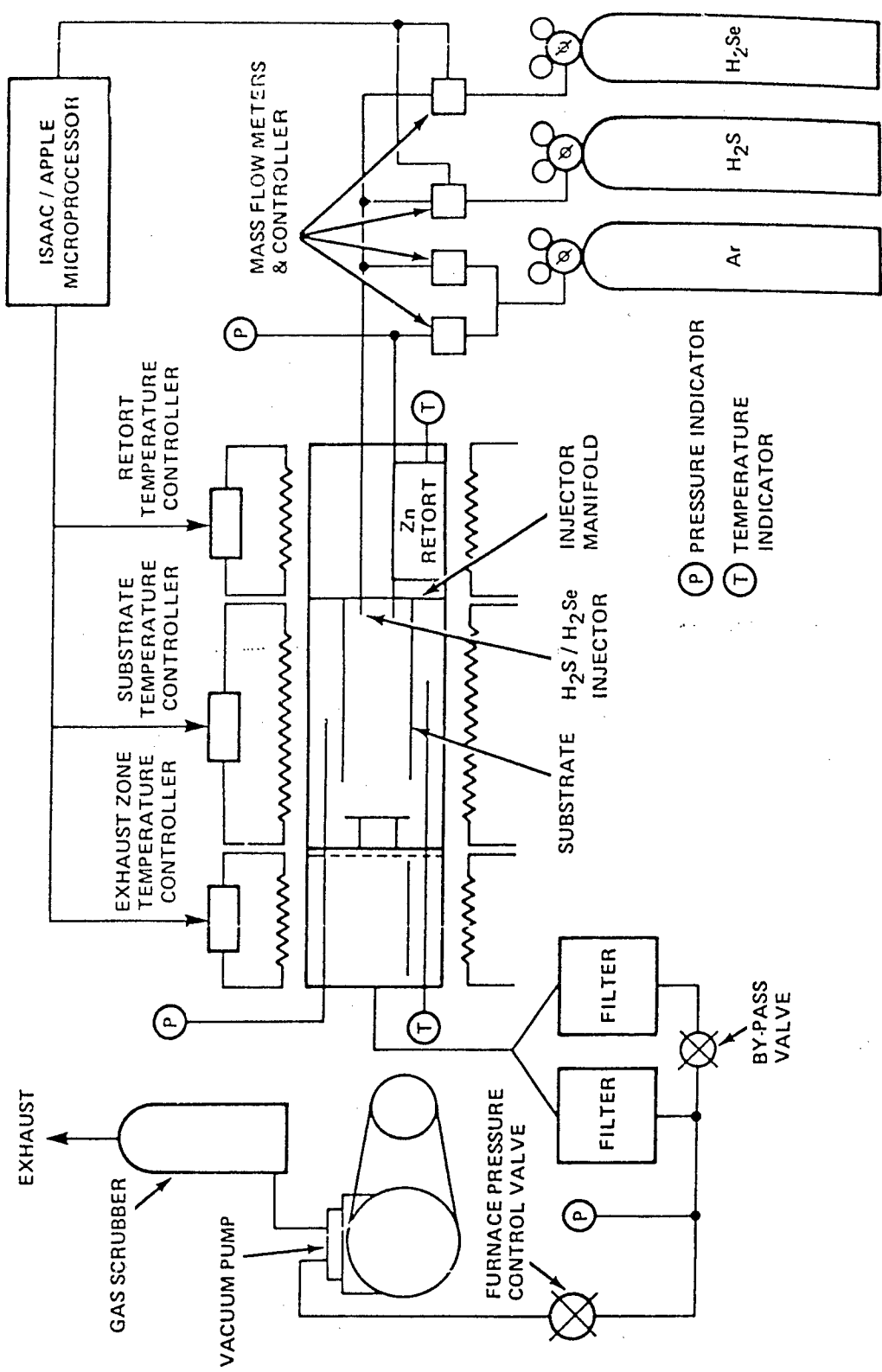


Figure 3. Schematic of research CVD apparatus used to deposit ZnS_xSe_{1-x} rugates.

adjusting the retort temperature and the argon carrier gas flow rate. The internal CVD setup is constructed of graphite and is contained in a quartz tube which becomes the vacuum chamber. The total pressure inside the reactor is maintained by a control valve which is used to throttle the vacuum pump. The flow rates, pressure and temperature of the furnace are controlled by microprocessors. During a deposition of a rugate filter the substrate temperature, total pressure, the Zn flow rate and total gas flow rate are all held constant while the ratio of the flow rates of H_2S and H_2Se , Q_{H_2S}/Q_{H_2Se} , is varied quasi continuously by the microprocessor which is programmed to produce the desired sinusoidal index profile. The mass flow controllers used for H_2S and H_2Se have response times of less than 1 second.

A computer program was written using Eqs. (6) and (7) and the model of the deposition process for ZnS_xSe_{1-x} described previously (see Eqs. (1) through (5)). This program allows one to input the desired filter characteristic and proceeds to calculate and control, in real time, the H_2S and H_2Se gas flow rates necessary to produce a specific rugate filter. The program uses the following step-by-step algorithm:

1. The rejection wavelength, bandwidth, optical density and number of flow changes per cycle (period) are specified as input.
2. Eqs. (6) and (7) are then used to calculate the index amplitude (Δn) and the number of cycles required to achieve the specifications given in Step 1.
3. Eqs. (1), (4) and (5) are then used to determine the flow rates of H_2S and H_2Se gas as a function of time.
4. The flow rates of H_2S and H_2Se gas are then controlled by a microprocessor (computer coupled to a D/A converter) by sending the appropriate voltage signal to the mass flow controllers.

Using the above model and apparatus we proceeded to perform rugate filter depositions. These films were grown on a number of different ZnS and

ZnSe substrates which ranged from 2 to 4 cm in diameter and 1.3 to 6 mm in thickness. Filters with rejection lines for varying from 7.5-11 μm were produced. Table 1 summarizes the deposition parameters for the experimental runs performed. In Run #1 we decided to use deposition conditions which were used in the previous GRIN work. A film thickness of ca. 358 μm was deposited in Run #1, however, during the first hour of deposition some pressure fluctuations did occur due to a clogged pressure control valve. These fluctuations in pressure usually result in poor material quality, i.e., inclusions and/or cloudy material. Three samples of ZnSe, each 25 mm ϕ by 3 mm thick, and three samples of ZnS, each 20 mm ϕ by 3 mm thick were polished and placed in the deposition zone prior to the run. All the samples were placed on the bottom mandrel plate (see Fig. 3) and located as shown in Fig. 4. All of the samples were cleaned in-situ by etching them in an H_2 atmosphere at 700 C for ca. 30 min. This treatment increases the adhesion of the films by removing any oxide/hydroxide layer from the ZnSe or ZnS surface. We have used this technique in the past and have found that it is necessary to achieve good adhesion when depositing pure ZnS and/or ZnSe onto either ZnS or ZnSe polished substrates. Figures 5 and 6 are transmission traces of rugate filters deposited in Run #1. Figure 5 is a trace of filter material taken from the exhaust (downstream) end of the mandrel plate and Fig. 6 is of sample 1-1A (see Fig. 4 for location) after polishing the film surface. Notice that in Fig. 5 the filter rejection wavelength is 10.2 μm which is close to the expected nominal value of 10 μm (see Table 1). The bandwidth is about 20%, which is considerably higher than the nominal value of 5%. Also, notice that the short-wavelength side of the filter tails off gradually while the high-wavelength side appear to be sharp. Considering only the high-wavelength side, the band-width is ca. 6% which is close to the expected value of 5%. We will discuss this phenomena in more detail below. Notice in Fig. 6 that the rejection wavelength is shifted to 7.8 μm and that there is an additional peak at ca. 6.9 μm . This result is not surprising and was expected for the CVD conditions used in this run. From the previous GRIN work we know that the gas phase composition of H_2S and H_2Se gas changes along the mandrel plates such that the gas is richer in H_2S toward the injector (upstream) end. Because of this the sinu-

TABLE 1.
Deposition and Filter Parameters for Zn_{1-x}Se_x Rugate Filter Runs

Run *	Nominal CVD Parameters			Nominal Filter Parameters			Comments	
	Substrate temperature (C)	Furnace Pressure (torr)	Flow Rate of H ₂ S and H ₂ Se (slpm)	Rejection Wavelength (μm)	Film Thickness (μm)	Bandwidth (% at 1/2 max)		Flow Changes per cycle
#1	710	30	0.30	10	358	5	20	Pressure fluctuations occurred early in deposition.
#2	710	30	0.15	10	384	3	20	Computer malfunction occurred a few hrs. into deposition; actual film thickness was ~ 100 μm.
#3	710	30	0.25	8	793	5	20	Flow rate of argon through injector was changing during deposition due to a clogged injector; run was aborted after 6 hrs.; actual film thickness was ~ 400 μm.
#4	710	30	0.25	8	990	4	20	No problems; material characterized.

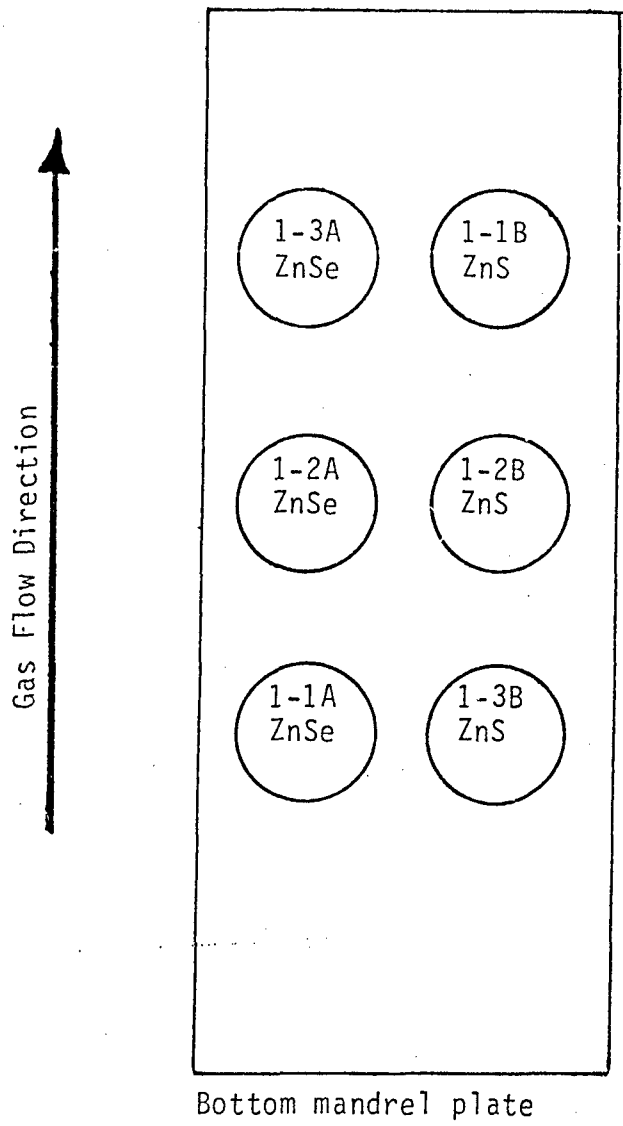
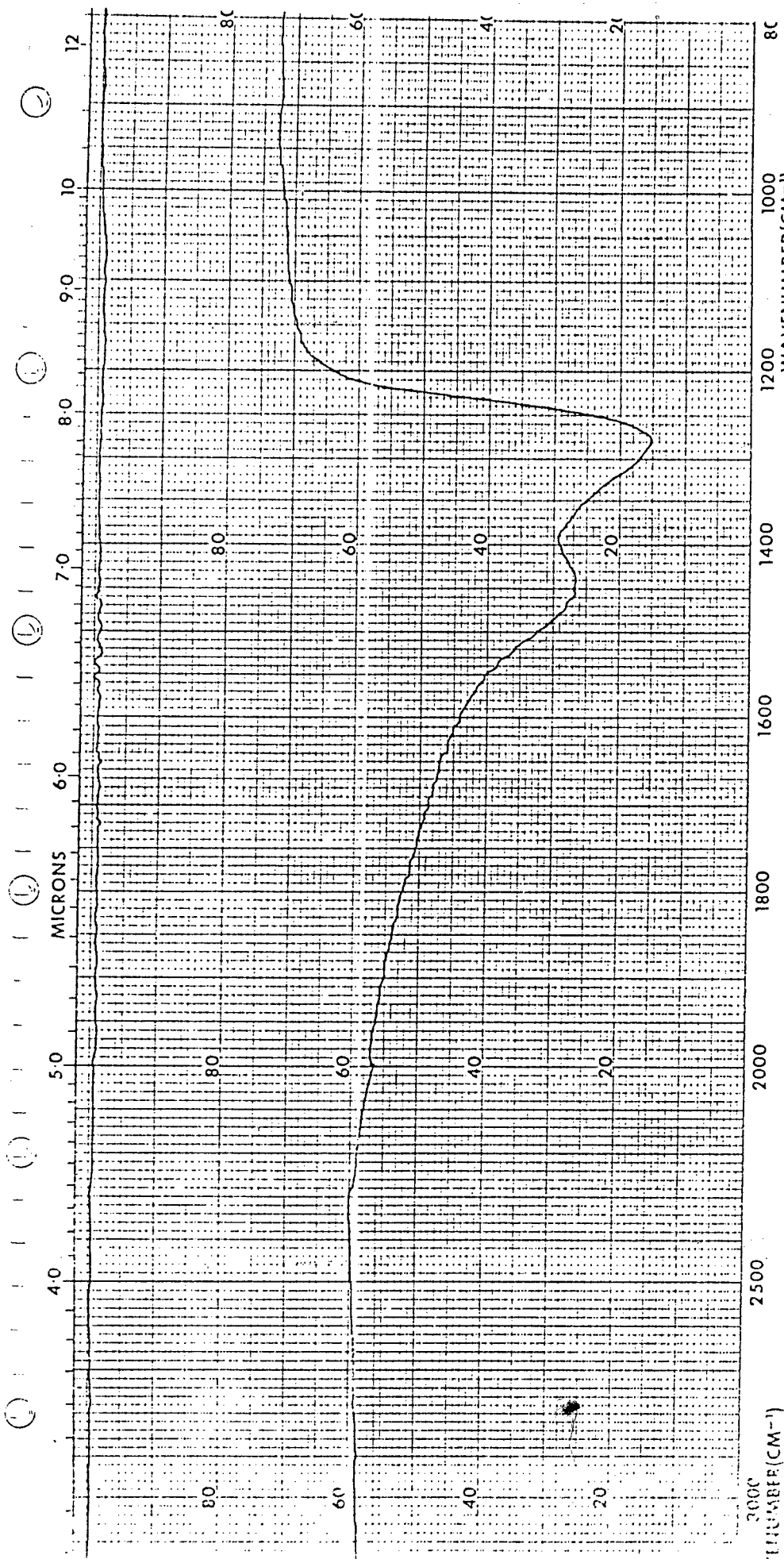


Figure 4. Location of ZnSe and ZnS substrates in Run #1.



SOLVENT _____ CONFIGURATION _____ CELL PATH _____ REFERENCE _____	REMARKS <i>Ni-Doped ZnSe</i>	SLIT PROGRAM _____ SCAN TIME _____ MULTIPLIER _____ TIME CONSTANT _____	T _____ A _____ SB _____ ORDINATE EXP _____	ABSCISSA _____ TIME DRIVE _____ OPERATOR _____
--	------------------------------	--	--	--

Figure 6. Transmission of ZnS_xSe_{1-x} rugate filter deposited on ZnSe sample 1-1A (see Fig. 4) during Run #1.

soidal variation in index will no longer be symmetric and the deposition rate will be lower near the injector end of the mandrel. Therefore, the rejection wavelength is reduced and the peak shape distorted.

In Run #2 we decided to reduce the deposition rate by a factor of two. This was accomplished by reducing the flow rates of H_2S and H_2Se gas (see Table 1) and Zn vapor. We also decided to reduce the peak-to-peak index variation (Δn) of the sinusoids to reduce the bandwidth from a nominal value of 5% to 3%. This deposition was scheduled to run for 12 hours, however, a computer malfunction (caused by power fluctuations) occurred a few hours into the deposition at which time the run was stopped. Because of this the film thickness, and therefore the OD of the filter, was considerably less than we had planned.

In Run #3 we decided to produce a thicker film to increase the OD and to shift the rejection wavelength from 10 to 8 μm to verify the deposition and rugate filter model, i.e., do changes in the computer input produce the corresponding changes in the filter. We also decreased the flow rates of the reactant gases to 0.25 slpm in order to maintain the time interval between flow changes. We concluded that a minimum of 4 seconds was needed between flow changes in order to produce the required compositional changes reproducibly, after taking into account the response time of the mass flow controllers and the time required for the reactant gases (H_2S and H_2Se) to travel from the mass flow controllers to the deposition zone.

Problems developed early in Run #3. After about an hour of deposition we noticed the argon flow through the injector began to decrease slowly. This was caused by clogged injector tip due to zinc vapor condensing on it. The day on which this run was performed was a particularly cold one. Since we were using tap water to cool the injector, which was very cold (5-10 C), zinc vapor condensed on the injector tip. Despite these problems we decided to continue the deposition for ca. 6 hrs., however, the flow conditions were changing during the run and, therefore, the results of this deposition are not definitive. We corrected this problem in Run #4 by installing a constant temperature recirculation bath

for the injector cooling water. This bath was maintained at 35 C during Run #4 and no clogging occurred during Run #4.

Despite the problems which occurred during Run #3, we were able to produce very high OD rugate filters in this run. We estimate that the rugate film thickness was ca. 400 μm for this aborted 6 hr. deposition. Again a large number of polished ZnSe and ZnS substrates were placed in the deposition zone prior to Run #3. The location of the samples are shown in Fig. 7. The larger circles represent a diameter of 40 mm and the smaller circles 25 mm. All of the samples were 3 mm thick and samples were mounted on both the bottom and top mandrel plates. Figure 8 is a transmission trace of sample 3-2A taken after Run #3. The curve labelled (1) is for gain of unity, (2) is at a gain of 2x and (3) at a gain of 3x. Curves 2 and 3 were generated by placing 50% and 33% filters in the reference channel of the spectrometer. From these curves we estimate the OD of this filter to be 1.9 - 2.3, the bandwidth (full at 1/2 max.) to be 20-25% and the rejection wavelength to be 7.75 μm . The nominal bandwidth and rejection wavelength for this deposition were 5% and 8 μm respectively. The rejection wavelength is within 3% of the nominal value, however, the actual bandwidth is considerably more than that predicted. This deposition clearly demonstrates that high OD $\text{ZnS}_x\text{Se}_{1-x}$ rugates can be produced by thick film depositions. As in Run #1, samples near the injector end of the mandrel plate, showed a shift in the rejection line to shorter wavelengths and poorer short wavelength transmission (asymmetric peak). This is illustrated in Fig. 9, a transmission trace for sample #3 - 9A from Run #3 (see Fig. 7 for location of sample) which was located near injector end (downstream) of the mandrel plate.

In order to verify that a periodic (sinusoidal) compositional change along the deposition axis was occurring in the film we cut and etched the surface perpendicular to the deposition axis for sample #3-1A. ZnS and ZnSe etch at different rates in HCl, therefore, a photograph of an etched surface of the film should show a periodic pattern due to this phenomena and the fact that the film composition changes periodically. This is shown in Fig. 10, a photograph of an etch surface of rugate film on sample #3-1A taken at a magnification of 2000x.

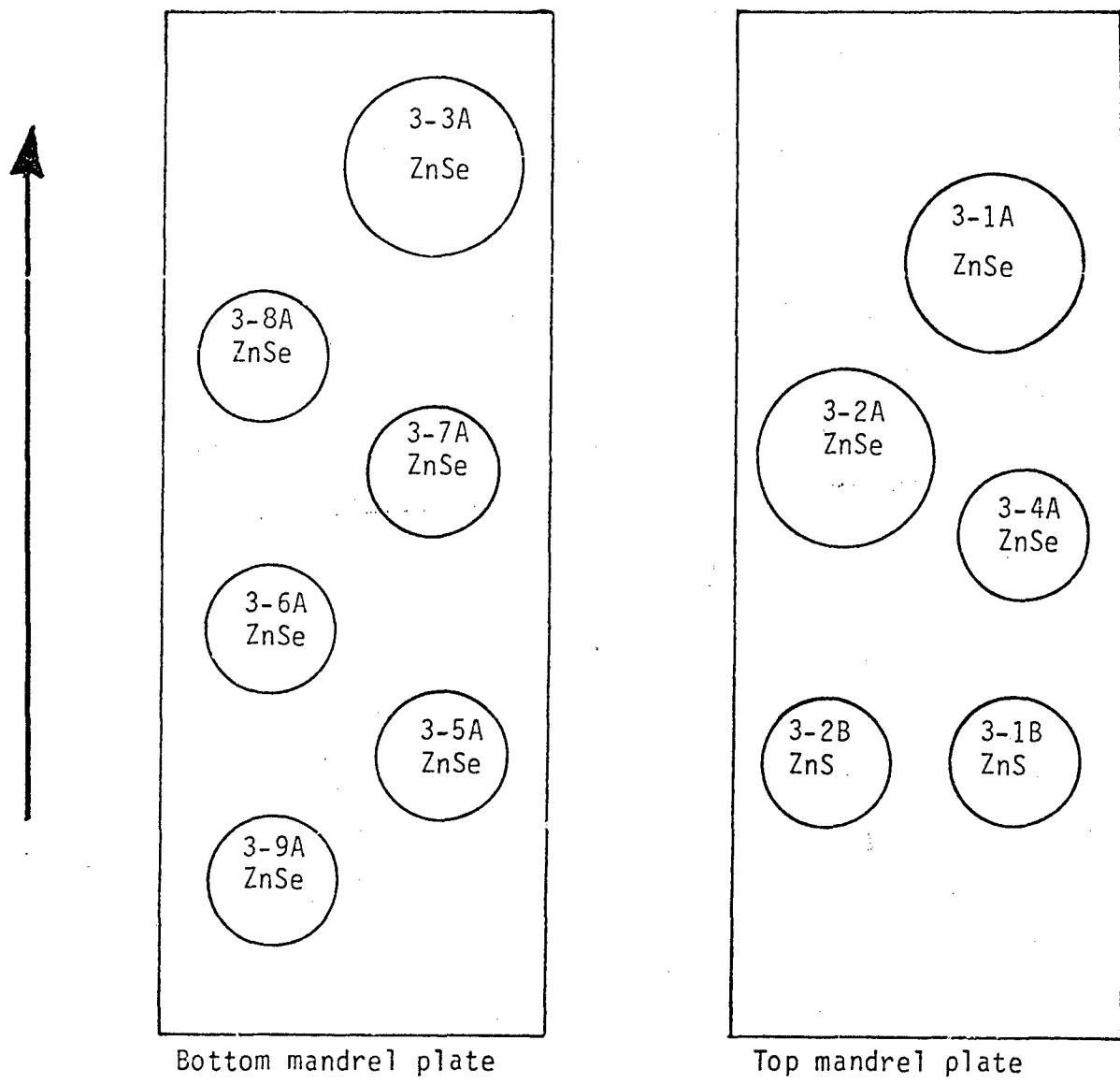
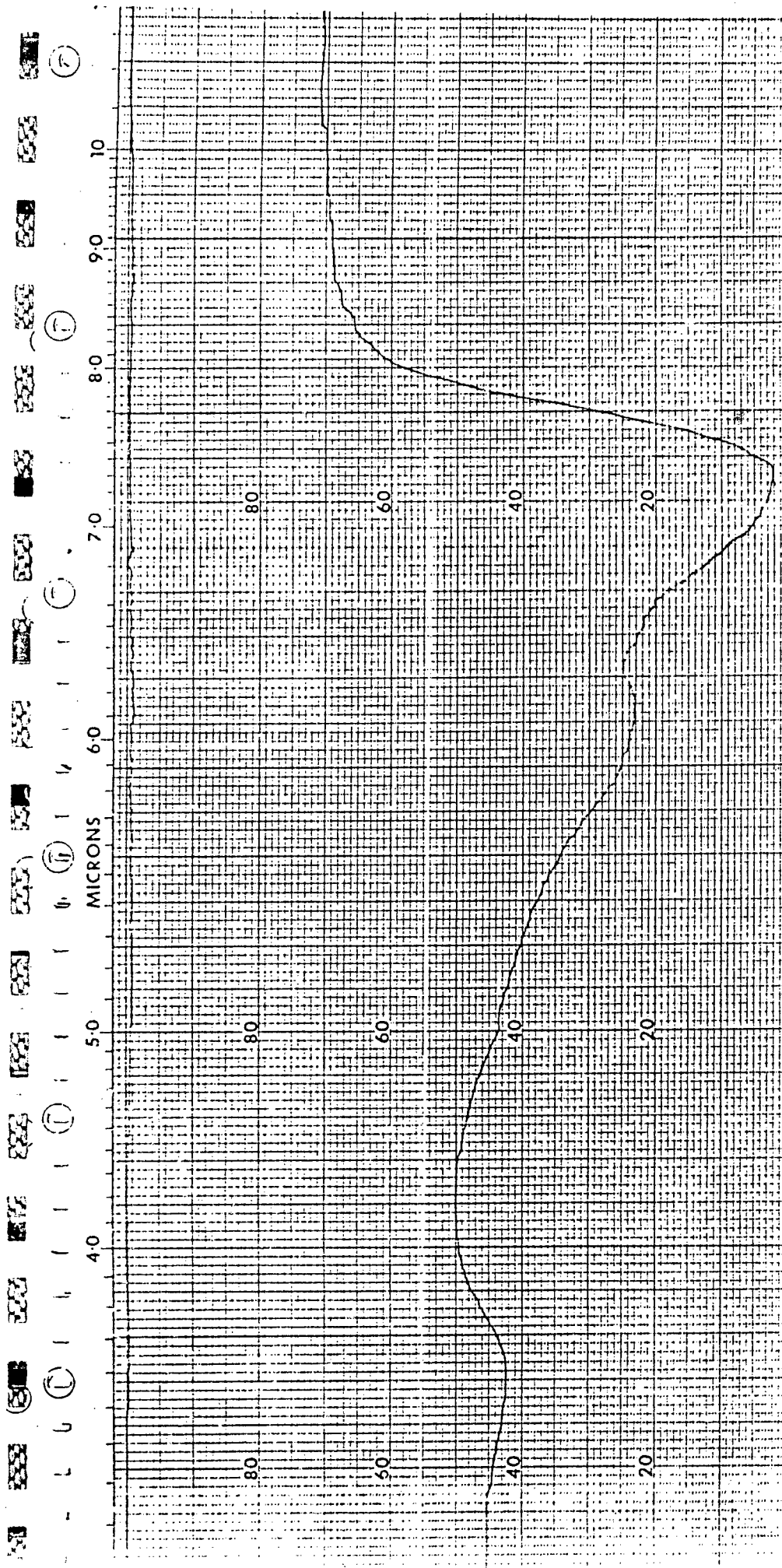


Figure 7. Location of ZnSe and ZnS substrates in Run #3.



3000 WAVENUMBER(CM ⁻¹)	2500	2000	1800	1600	1400	1200 WAVENUMBER(CM ⁻¹)	1000		
SOLVENT	REMARKS <i>Location: Bottom - non-fid end</i>						T	A	SE
CONCENTRATION	$\bar{c} = 0.1646$						SLIT PROGRAM	ABS	TIM
CELL PATH							SCAN TIME	ORDINATE EXP	
REFERENCE							MULTIPLIER		
							TIME CONSTANT		OFF

Figure 9. Infrared transmission of rugate filter grown on sample #3-9A during Run #3. See Fig. 7 for location of sample indeposition zone.

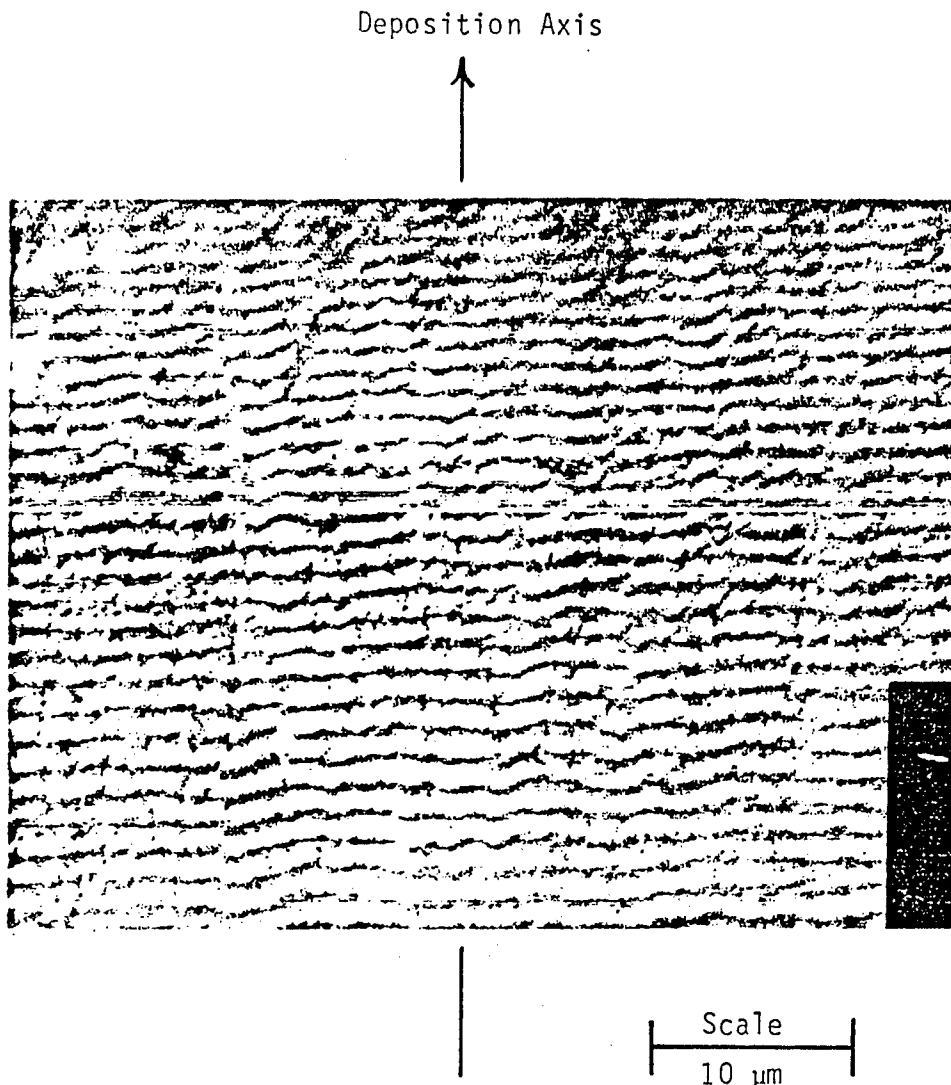


Figure 10. Photograph of an etched surface of rugate filter parallel to deposition axis on sample #3-1A in Run #3. Note the periodic line pattern showing that the concentration of ZnSe and ZnS is changing periodically along the deposition axis.

Notice the periodic line pattern along the deposition axis. This clearly demonstrates that the concentration of ZnS and ZnSe in the alloy ZnS_xSe_{1-x} is changing periodically along the deposition axis. Notice that the lines are fairly evenly spaced, but, they are "bumpy". This bumpy or non-uniform growth is common in thick CVD deposits.⁶ From this photograph we determine the physical period to be ca. 1.6 μm . This corresponds to a rejection wavelength of 7.4 μm which is close to the measured rejection wavelength of the 7.8 μm for the sample.

Run #4 (see Table 1) was essentially a repeat of Run #3, except that the injector coolant water was maintained at 35 C and the nominal bandwidth was reduced to 4%. Run #4 was a 16-hour deposition with no apparent problems. A number of ZnSe and ZnS substrates were placed in the deposition zone prior to Run #4 and the location of these samples is given in Fig. 11. Again the larger circles represent 40 mm diameter samples and the smaller circles 25 mm diameter samples. All samples were 3 mm thick. Figure 12 is a transmission trace of sample #4-3A taken after Run #3. The curve labelled (1) is for gain of unity, (2) is at gain of 2x and (3) at a gain of 3x. From Fig. 12 we estimate the OD of this filter to be ca. 2.3, the bandwidth to be 22-26% and the rejection wavelength to be 7.6 μm . As in previous filter depositions the actual bandwidth is much higher than the predicted one. Also notice in Fig. 12 that there appears to be two peaks at the base of the filter. We decided to investigate the filter characteristic as a function of thickness by lapping and polishing an as-deposited filter to reduce the thickness and then examining its transmission. This is shown in Fig. 13. Curve 2 is the as-deposited film on sample #4-1A which had a measured thickness of 900 μm and Curve 1 is the same with the film thickness lapped and polished to a thickness of 250 μm . Notice, that the bandwidth of the thinner film (Curve 1) is much narrower than for the thick film, i.e., BW = 10% for the thin film and 23% for the thick film. Also notice that the rejection peak is shifted to shorter wavelengths for thin film and that the short wavelength transmission is much improved. This data suggest that the growth morphology and/or growth rate may be changing with film thickness. This should be evident by observing the microstructure of the film. In order to do

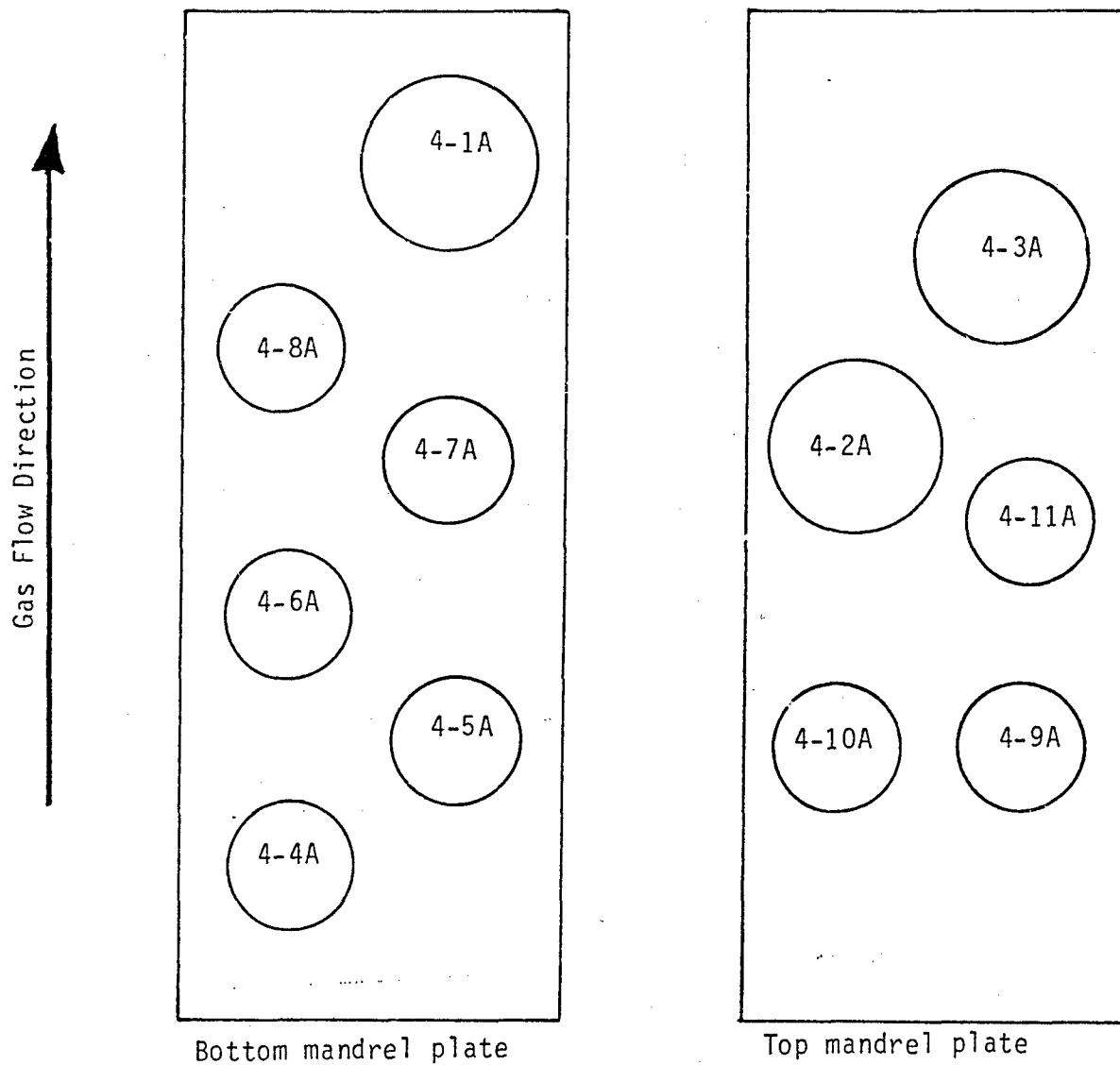
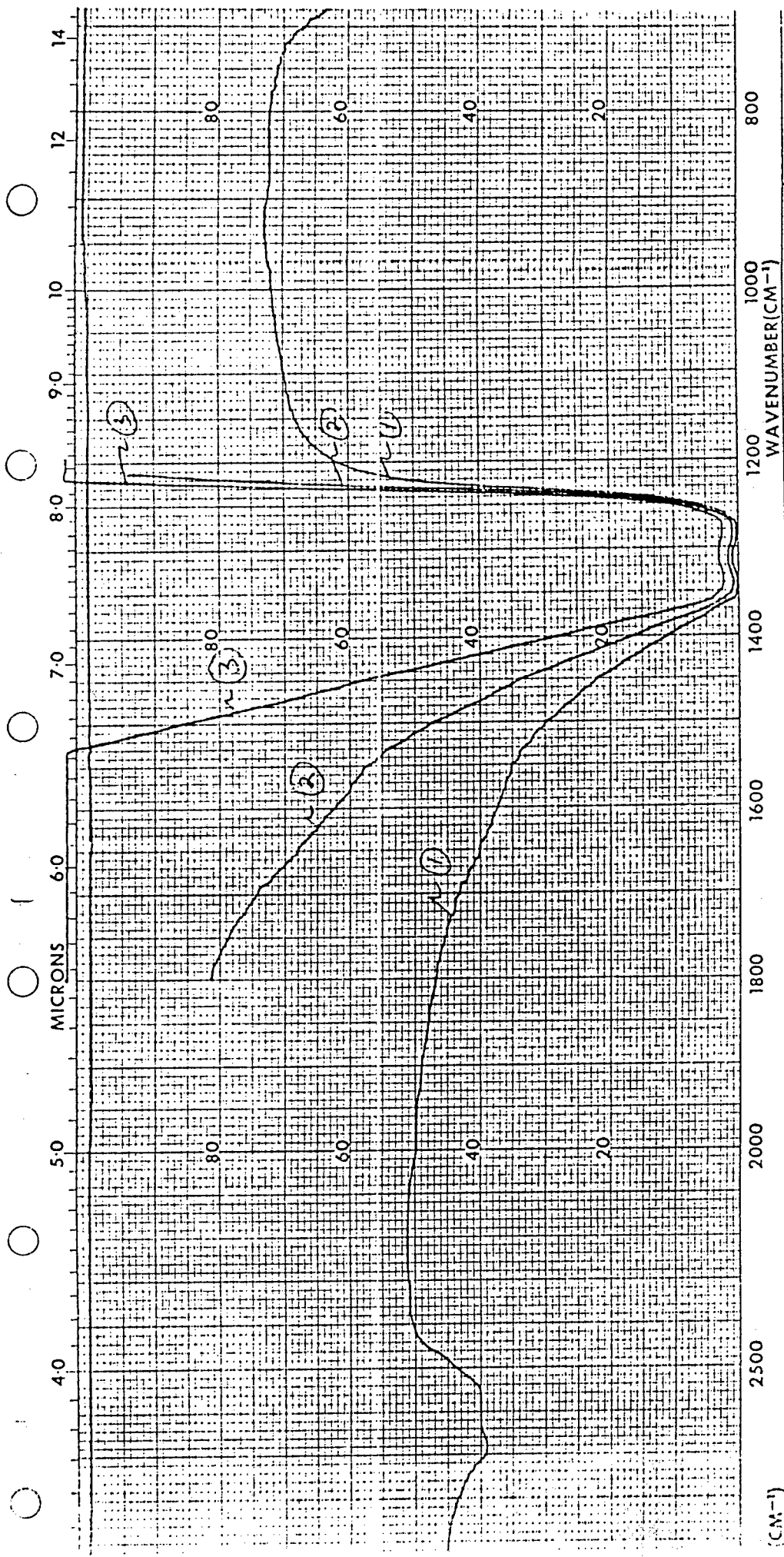
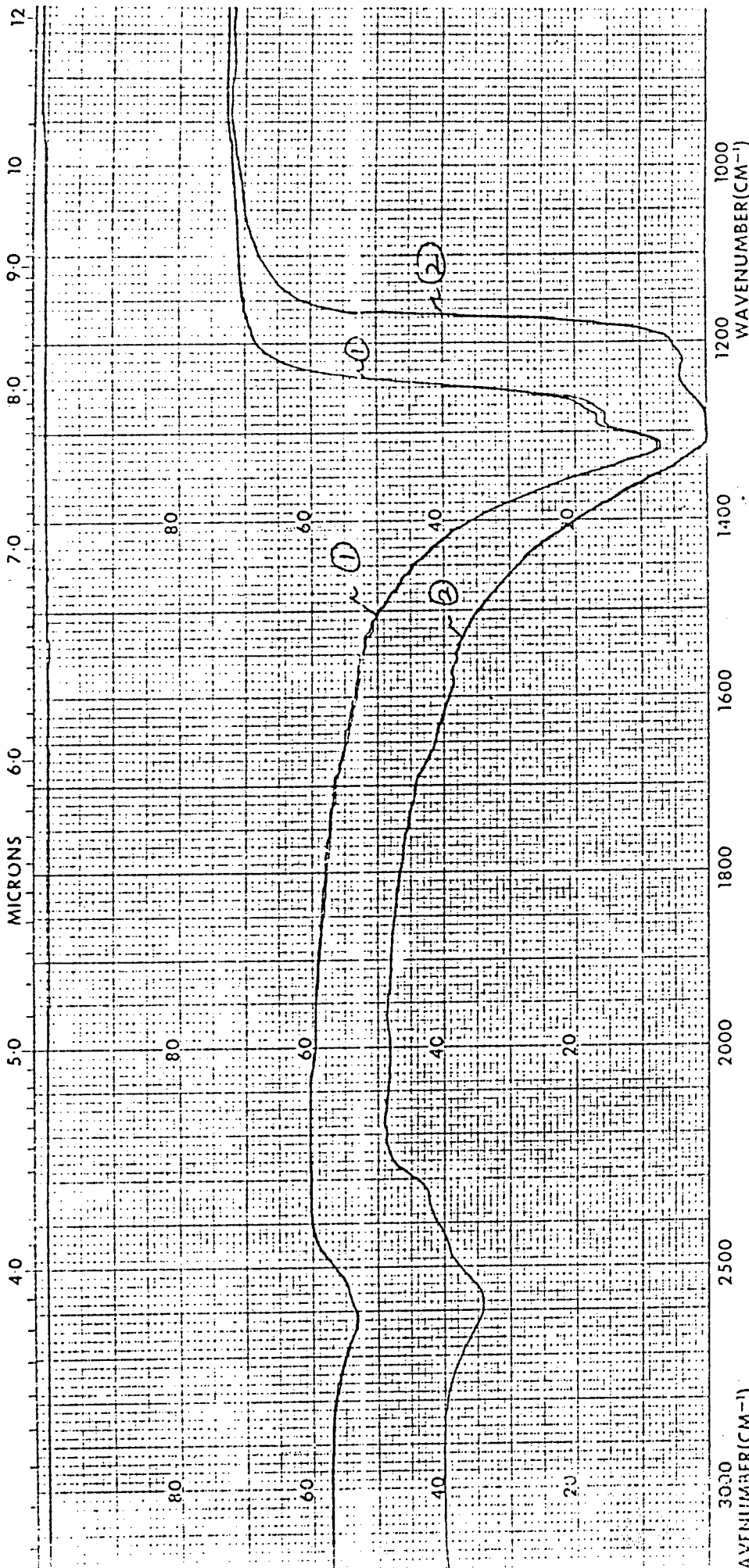


Figure 11. Location of ZnSe substrates in Run #4.



IT	WAVENUMBER (CM ⁻¹)	ABSCISSA EXP.
TITRATION	800	TIME DRIVE
TH	1000	OPERATOR
ICE	1200	WAVENUMBER (CM ⁻¹)
	1400	800
	1600	1000
	1800	1200
	2000	1400
	2500	1800
		2000
		2500
		3000
		3500
		4000
		4500
		5000
		5500
		6000
		6500
		7000
		7500
		8000
		8500
		9000
		9500
		10000
		10500
		11000
		11500
		12000
		12500
		13000
		13500
		14000
		14500
		15000
		15500
		16000
		16500
		17000
		17500
		18000
		18500
		19000
		19500
		20000
		20500
		21000
		21500
		22000
		22500
		23000
		23500
		24000
		24500
		25000
		25500
		26000
		26500
		27000
		27500
		28000
		28500
		29000
		29500
		30000
		30500
		31000
		31500
		32000
		32500
		33000
		33500
		34000
		34500
		35000
		35500
		36000
		36500
		37000
		37500
		38000
		38500
		39000
		39500
		40000
		40500
		41000
		41500
		42000
		42500
		43000
		43500
		44000
		44500
		45000
		45500
		46000
		46500
		47000
		47500
		48000
		48500
		49000
		49500
		50000
		50500
		51000
		51500
		52000
		52500
		53000
		53500
		54000
		54500
		55000
		55500
		56000
		56500
		57000
		57500
		58000
		58500
		59000
		59500
		60000
		60500
		61000
		61500
		62000
		62500
		63000
		63500
		64000
		64500
		65000
		65500
		66000
		66500
		67000
		67500
		68000
		68500
		69000
		69500
		70000
		70500
		71000
		71500
		72000
		72500
		73000
		73500
		74000
		74500
		75000
		75500
		76000
		76500
		77000
		77500
		78000
		78500
		79000
		79500
		80000
		80500
		81000
		81500
		82000
		82500
		83000
		83500
		84000
		84500
		85000
		85500
		86000
		86500
		87000
		87500
		88000
		88500
		89000
		89500
		90000
		90500
		91000
		91500
		92000
		92500
		93000
		93500
		94000
		94500
		95000
		95500
		96000
		96500
		97000
		97500
		98000
		98500
		99000
		99500
		100000

Figure 12. Infrared transmission of Zn_SSe_{1-x} rugate filter on ZnSe substrate sample #4-3A in Run #4. See Fig. 9 for location of sample in deposition zone. Curve ① is for a gain of unity; Curve ② gain is 2x; Curve ③ gain is 3x.



SCIENT	SUIT PROGRAM	T	ABSCISSA
CONCENTRATION	SCAN TIME	A	TIME DR
CELL PATH	MULTIPLIER	ORDINATE EXP	OPERAT
REFERENCE	TIME CONSTANT		

REMARKS
 (1) Film thickness ~ 250 μm
 (2) Film thickness ~ 900 μm

Figure 13. Infrared transmission of Zn_xSe_{1-x} rugate filter on ZnSe substrate samples #4-1A in Run #4. Curve 1 is for a film thickness of 250 μm and Curve 2 is for a thickness of 900 μm.

this we cut, polished and etched sample #4-3A and observed the microstructure along the deposition axis. This is shown in Fig. 14. Notice that the dark - light lines, which show the periodic structure in the film, are fairly evenly spaced, however, they suddenly change direction as noted in Fig. 14 and form a "cone" structure. At the base of the cone where this sudden change in growth occurs, notice that the lines form a circle, as if suddenly an impurity (small particle) has been swept onto the surface and is now being coated. We believe that this phenomena is the cause of the asymmetric peak shapes and large bandwidths we have observed in this film. This suggests that a cleaner CVD system is needed. We discuss this in more detail in the next section.

Deposition Axis



Note origin of sudden
change in growth morphology.

ZnS_xSe_{1-x} rugate film.

ZnSe substrate

Scale
30 μm

Figure 14. Photograph of etched surface, parallel to deposition axis, for sample #4-3A. Note the dark-light lines showing the periodic structure of the film and sudden change in growth morphology (cone structure). We believe this phenomena is due to impurities being swept onto the surface of the film during growth.

3.0 DISCUSSION OF RESULTS

Although this Phase I program was highly successful, several technical issues, which became apparent during this work, require further investigation. These include: (1) The measured bandwidth of the filters produced were considerably larger than the predicted ones. (2) The shape of the rejection peaks were asymmetric, i.e., the long wavelength edge was very sharp and the low wavelength edge tailed off gradually. Also, in some cases there were multiple minima at the base of the rejection band. (3) The rejection wavelength and shape of the filters varied along the deposition zone.

Several factors can contribute to widening of the rejection band such as non-uniform growth over the substrate surface, a change in the growth rate during the deposition which results in a change in the period, and changes in growth morphology which occur during the film deposition, i.e., sudden localized changes in growth caused by either gas phase particles forming, contaminants acting as active growth sites and/or small particles being swept onto the film surface during growth.

All of the above phenomena can be investigated experimentally and eliminated and/or reduced. For example, in Fig. 14, a photograph taken of an etched film produced in this Phase I, shows what appears to be a sudden change in growth morphology due to a small (1-2 micron) particle swept onto the surface of the film during growth. If this is the case, steps can be taken to "clean-up" the CVD reactor to prevent this. One possible source of particle contamination is the zinc metal and graphite zinc retort, both of which could be eliminated by using metal-organics, such as dimethylzinc or diethylzinc as sources of Zn. Both of these chemicals are available in high purity. Also steps can be taken to clean the plumbing by using highly polished stainless steel (ss) lines instead of standard ss tubing that we are now using.

An important point worth noting about the rugate filters produced in this Phase I effort is the apparent absence of side-bands. Most rugate filters

that have been produced to date show appreciable side-bands which reduce the off-band transmittance and is therefore undesirable. Quarterwave dielectric filters also exhibit side-bands.

4.0 CONCLUSIONS AND RECOMMENDATIONS

This work has established the feasibility of producing high-optical-density ZnS_xSe_{1-x} rugate filters. Rugate filters with rejection lines from 7 to 11 μm , bandwidths of 20-26% and optical densities as high as 2.3 have been produced by a scalable low pressure chemical vapor deposition process (CVD) involving a reaction between zinc vapor and H_2S and H_2Se gas. These rugate filters have been successfully deposited onto polished ZnS and ZnSe with good adhesive. An analytical model of the CVD process coupled with an approximate theoretical treatment of rugate filters was used to develop a computer program, which in turn, was used to control the CVD process to produce specific rugate filters. Because of the success of this modest Phase I effort and the importance of this technology development to the overall success of SDI, we strongly recommend that this work be continued.

REFERENCES

1. C. M. Phillippi and J. Davidson, "Rugate Filters, A New Approach to Laser Vulnerability, Effects and Hardening, Oct. 1982.
2. W. E. Johnson, C. L. Strecker and J. E. Davidson, "Preparation of a Silicon-Germanium Rugate Filter", Proc. of 5th DoD Conference on Laser Vulnerability, Effects and Hardening, Oct. 1982.
3. K. Kogler, E. Rea, J. Stubbs, N. Murarka and C. M. Phillippi, "Rugate (Graded Refractive Index) Filter", Proc. of 5th DoD Conference on Laser Vulnerability, Effects and Hardening, Oct. 1982.
4. M. A. Pickering, R. L. Taylor and D. T. Moore", Gradient Infrared Optical Material Prepared by a Chemical Vapor Deposition Process", Appl. Opt. 25 (19) (1986) 3364-72.
5. J. A. Dobrowolski and D. Lowe, "Optical Thin Film Synthesis Program Based on the Use of Fourier Transforms", Appl. Opt. 17 (19) (1978) 3039-50.
6. W. A. Bryant, J. Mat. Sci. 12 (1977) 1285-306.